

**Immobilisation of BaSO<sub>4</sub>: Phases and microstructure of OPC-BaSO<sub>4</sub> system cured at an elevated temperature -11012**

O.H. Hussein, M. Ojovan, H. Kinoshita

Department of Materials Science and Engineering, University of Sheffield, Mappin Street, Sheffield S1 3JD, UK

**ABSTRACT**

In many countries, significant radioactive contamination may occur in the oil and gas industrial processes due to the solid - precipitates containing natural radioactive elements, commonly known as Naturally Occurring Radioactive Materials (NORM). The most of the radioactivity is dominantly from <sup>226</sup>Ra and <sup>228</sup>Ra, and these isotopes co-precipitate with the barium as sulphate to form (Ba, Ra) SO<sub>4</sub> solid solution on the inner surface of the pipes, tanks and other facilities. Consequently, such radioactive waste stream needs to be disposed, typically as a low level radioactive waste (LLW). Cementitious, or cement-based, waste forms are commonly used worldwide for storage and disposal of LLW and intermediate level waste (ILW), hazardous and mixed wastes. Hardened ordinary Portland cement (OPC) paste provides an excellent medium for immobilisation of LLW because of its durability and flexibility as a nuclear waste immobilising matrix.

In the present study, OPC system with additions of a simulated radioactive waste stream of BaSO<sub>4</sub> with different waste loading (0%, 6%, 12%, and 18%) was studied. The systems were cured at elevated temperatures to simulate the high temperatures generated at the centre of large volumes of hydrating cementitious material, which can affect the rate of hydration and the phases and microstructure formed. X-ray diffraction (XRD), Thermogravimetric analysis (TGA), and scanning electron microscopy (SEM) were utilised to study the phases formed in the system and microstructure as well as the effects of BaSO<sub>4</sub> contents on these properties of the system. The greater amounts of barite (BaSO<sub>4</sub>) were fixed during the hydration of OPC with w/s 0.53 and that the basic cement hydration was not disturbed by addition of 18% of the barite waste into cement paste. The small addition of BaSO<sub>4</sub> showed a greater development in the hydration phases while the larger addition of BaSO<sub>4</sub> showed a less content of hydration phases. BaSO<sub>4</sub> appears to remain unreacted in all OPC matrixes. The addition of the BaSO<sub>4</sub> changed the pore structure of the cement paste.

**INTRODUCTION**

**Overview**

In many countries, significant radioactive contamination in the oil and gas industrial processes occurs due to the solid precipitates scale containing natural radioactive elements, commonly known as NORM, which are by-products present in varying concentrations in hydrocarbon reservoirs [1]. The radioactivity in the scale primarily comes from radium and its daughter nuclides [1, 2, 3, 4, 5, 6, 7, 8]. Because of the chemical similarity of radium and barium, radium naturally accumulates in the scale matrix of barium sulphate BaSO<sub>4</sub>, which then becomes radioactive and therefore, requires an appropriate handling [7]. The scales obtained from piping decontamination are most often classified as low level radioactive waste [9, 10]. Radioactive waste is typically immobilised to provide higher safety of handling, transportation, and hardened Portland cement paste provides an excellent medium for immobilisation of low level radioactive wastes [11]. The results of previous work by Read et al. [2] has suggested that composite cement system of Portland cement - pulverised fly ash - metakaolin [OPC-PFA-MK] could be a preferred encapsulate for BaSO<sub>4</sub>-containing NORM. The present paper reports the results obtained from the basic study for OPC-BaSO<sub>4</sub> wasteform. This study was carried out, because the data currently available in the literature on this system is limited, especially for suitable formulation and phases formed.

**Scale formation**

The formation of scales in the oil and gas industry is due to the chemical-physical processes which take place in the reservoir's production water [12]. Figure 1 shows a schematic diagram of scale formation. It consists of following steps (i) Water injection: in order to keep the oil production stable and also, to maintain the well integrity with the production time. It is necessary to inject seawater (contains ions of sulphate SO<sub>4</sub>) into the wells; (ii) Mixing: then seawater is mixed with formation water (contains ions of the Alkali Earth elements, including radium); (iii)

Precipitation: as the mixture water reach the surface, pressure, temperature and pH can change leading to the radium isotopes ( $^{226}\text{Ra}$  and  $^{228}\text{Ra}$ ) to precipitate [1, 2, 3, 5].

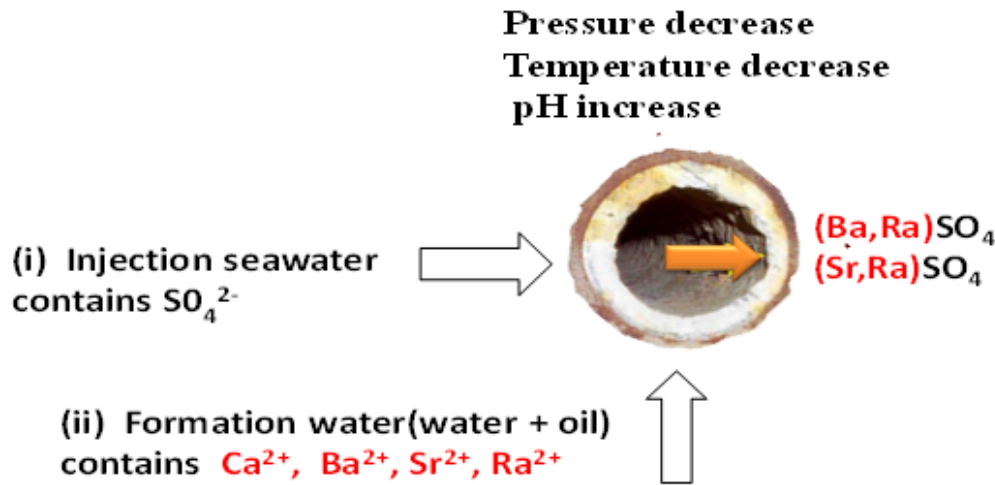
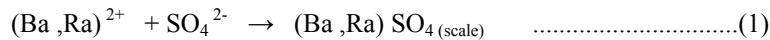


Figure 1 Mechanism of radioactive scale formation inside of oil pipes

Usually radium co-precipitates with barium and strontium salts to form  $(\text{Ba}, \text{Ra})\text{SO}_4$  and  $(\text{Sr}, \text{Ra})\text{SO}_4$  as shown in equation 1 and 2 [1, 2, 3, 5].



The affinity of the radium ion with barium and strontium salts crystal lattices is due to the similarity of their valence and ionic radius [6, 13, 14, 15, 16, 17]. A study by Al-Masri and Aba [1] reported the correlation among the concentration of elements, Ba, Sr and Ra in scale. The concentration of radium increases as the concentration of barium and strontium increase. Therefore, larger amounts of precipitation in barium and strontium sulphate will lead to a larger amount of radium co-precipitation [18].

### Cementation of $\text{BaSO}_4$ NORM Scale

Scale containing NORM can be classified as LLW depending on Ra concentration, reaches up to 15000 Bq/g [19]. In general, the interaction between the hardened cement matrix and the waste is strongly dependent on the chemical reactivity of the waste and cement paste and hydration reactions involving the waste. These areas have generally been reviewed by Glasser 1992[21], Gougar et al. [22], and Sharp et al. [11] among others. By controlling conditions during hydration (i.e. curing temperature or composite cement composition) it is possible to form an efficient immobilising matrix with desirable microstructure, physical properties and internal chemical environment for specific ion encapsulation, and helps to determine whether the active elements remain in their original form or if they are incorporated into cement hydration products.  $\text{BaSO}_4$  salt dissolve only 2.22mg/L in cold water [20]. Therefore, its reaction with cement is expected to vary little due to the strong bond between barium sulphate and its insolubility, but little work has been done concerning Ra-containing  $\text{BaSO}_4$  in the composite cement systems. The aim of our work was to analyse characteristics and microstructure on cementitious wasteform containing  $\text{BaSO}_4$  simulate as a function of waste loading. The challenge is to embed as much as possible NORM scales into cementitious wasteform while not compromising its durability and long-term stability.

**EXPERIMENTAL PROCEDURE**

**Materials**

A commercial OPC was provided by Castle Cements product UK. The composition of OPC on oxide basis is shown in Table 1. The cement had a fineness of 352 m<sup>2</sup>/kg Blaine. BaSO<sub>4</sub> powder was sourced from Acros organics to simulate the waste stream.

Table 1 composition of the OPC powder [23].<sup>(23)</sup>

Component	CaO	SiO <sub>2</sub>	Al <sub>2</sub> O <sub>3</sub>	Fe <sub>2</sub> O <sub>3</sub>	MgO	SO <sub>3</sub>	K <sub>2</sub> O	Na <sub>2</sub> O	ignite less	Total
<b>Wt%</b>	64.58	20.96	5.24	2.61	2.09	2.46	0.59	0.28	0.73	99.9

**Mix formulation and curing**

The formulations of the samples are given in Table 2. The water to solid ratio for all samples was 0.53 on a mass basis which is the same ratio for a previous study by Read [2]. The OPC and BaSO<sub>4</sub> were weighed and mixed according to the ratios shown in the Table targeting total of 25 g. The mixed powders were placed in plastic containers (a diameter of 30 mm, a height of 120 mm and a wall thickness of 2 mm). Then the powder and 13.25 g of water were added and mixed manually at room temperature, for around 2 minutes, then mixed for 5 more minutes using a Whirh Mixer. The samples were clearly labelled and stored in environmental chamber at 40 °C, RH.95%. After 28 days, samples were demoulded from the plastic pots and were broken into smaller pieces and submerged in acetone for three days to arrest hydration reactions. The samples were then dried and desiccated under vacuum to drive off the acetone. Samples were stored in sealed containers prior to analysis.

Table 2 details of the cement samples prepared

	OPC, wt%	BaSO <sub>4</sub> , wt%	Solid Total, wt%	Solid total weight, g	Water, g	Curing time	Temp., °C	RH <sup>1</sup> , %
1	100	0	100	25	13.25	28 days	40	95
2	94	6	100					
3	88	12	100					
4	82	18	100					

**Analysis**

**X-ray diffraction (XRD)**

XRD was the main technique used to identify the presence of crystalline compounds in the studied samples. A Siemens D500 X-ray diffractometer with monochromatic Cu K $\alpha$  radiation with a wavelength of 1.5405 Å was operated at voltage of 40 kV and current of 30 mA. The 2 $\theta$  scans were used to examine the samples over the range of 5-65° 2 $\theta$  with a step size of 0.02° and scanning speed of 2°/min. The samples were prepared by initially crushing samples using a percussion mortar then grinding to a fine powder by an agate mortar and pestle, sieving by using brass sieve, to a particle size less than 63 μm and placed in an aluminium sample holder. The resulting traces were interpreted using the ICDD files in the standard JCPDF card and STOE WinXPOW software.

**Thermogravimetry (TG)**

TGA was used to identify phases present in each of the samples from the dehydration and decomposition temperatures by determining the changes in sample mass during the heating. The measurements were carried out using a Perkin Elmer Pyris 1 TGA. Powder was obtained crushing specimens by an agate mortar and pestle. Samples were ground to <63μm, and approximately 40 mg of sample was weighed to within ± 0.0001g of error

<sup>1</sup> RH = relative humidity

using an electronic microbalance and placed in an alumina crucible in the furnace. The samples were heated under flowing nitrogen atmosphere. A uniform heating rate of 10 °C/min from room temperature up to 1000 °C was chosen. The results were analysed based on the data in the literature [24], a summary of which can be found in Table 3.

Table 3 Location (°C) and origin of in TG for cement phases [25]:

C-S-H	Ettringite	Monosulfate	Calcium hydroxide	Calcium carbonate
110-120	130-140	180-210	480-520	600-700

### **Scanning electron microscopy (SEM)**

SEM was used to study microstructure of the samples. SEM images were taken by JEOL electron microscope; JSM 6400. The acceleration voltage was 20 KeV with a spot size of 9. Most of the samples investigated with SEM were carried out in backscattered electron imaging mode (BSE), which shows the distribution of elements in different contrast. Samples were prepared by mounting a small solid portion in cold set epoxy resin in a cylindrical plastic mould. The epoxy resin was poured over the samples and leaving under vacuum to fill as many pores as possible. The samples were removed from the vacuum after approximately 15 minutes and left for 24 hours to harden before grinding manually with grinding papers of 250, 400, 800 and 1200 grit. The observation surfaces were then polished with 6, 3, 1, and 1/4 µm diamond pastes, and coated finally with carbon using an Edwards 'speedivac' carbon coating unit and silver dagged to make them electrically conductive before being analysed in the microscope.

## **RESULTS AND DISCUSSION**

### **XRD results**

Figure 2 shows the XRD traces for samples after 28 days with different waste loading of BaSO<sub>4</sub> (0, 6, 12, and 18%). The figure also indicates XRD pattern for pure BaSO<sub>4</sub> for comparison.

The main crystalline phases detected for hydration of pure OPC for 28 days were calcium hydroxide (P) and Monosulfate (Ms). Some unreacted alite (A) and belite (B) were also present suggesting that the system had not completely hydrated. Furthermore, some carbonation seems to have occurred to form calcium carbonate (C). The XRD traces for samples containing BaSO<sub>4</sub> also indicated clear peaks of BaSO<sub>4</sub> (Bs). Majority of BaSO<sub>4</sub> added seems remained as expected. XRD traces for the samples showed a gradual change in the peak intensity BaSO<sub>4</sub>; as the loading of BaSO<sub>4</sub> increases, the intensity of BaSO<sub>4</sub> peaks became higher.

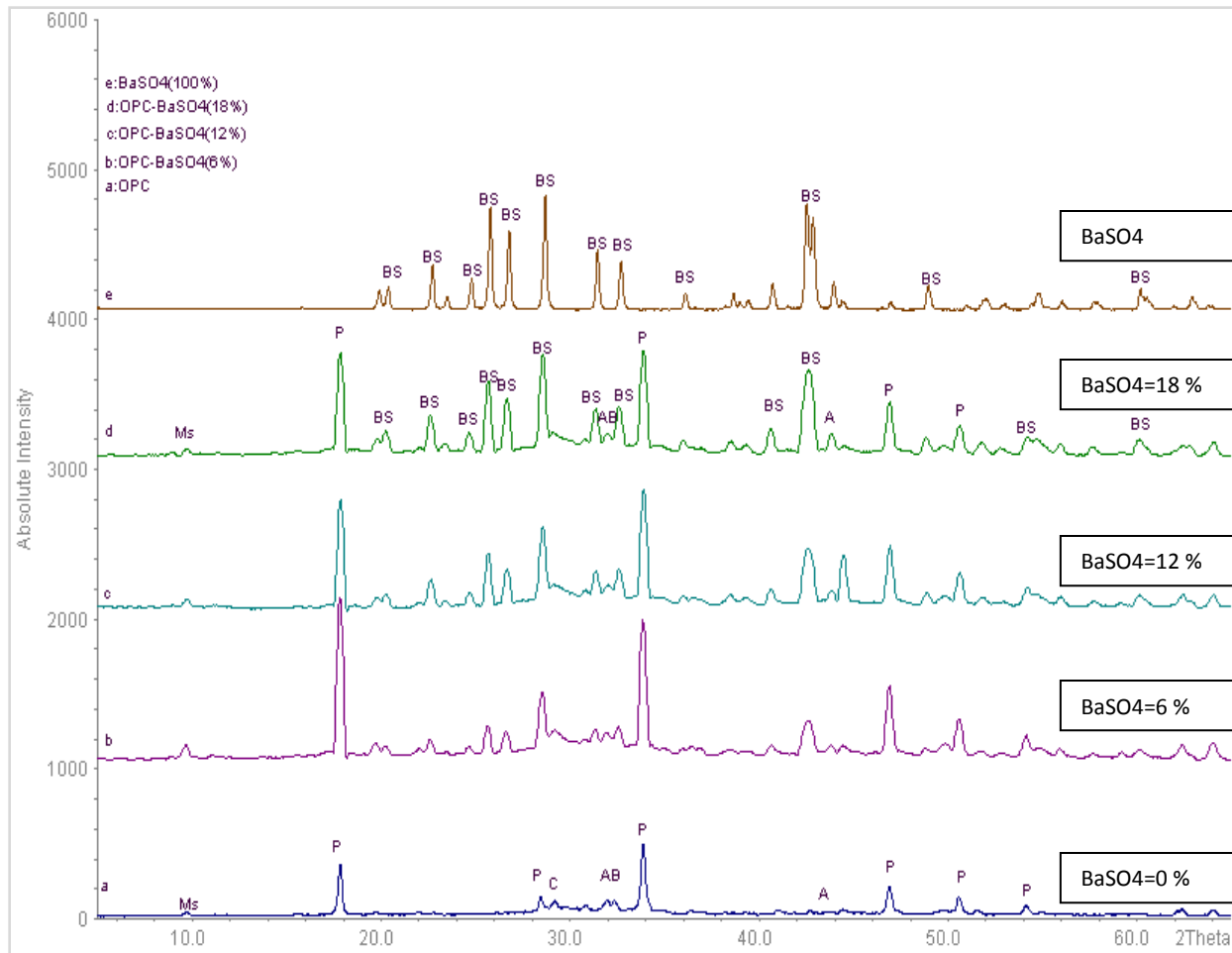


Figure 2 comparison of XRD traces for OPC-BaSO<sub>4</sub> system cured at 40°C for 28 days w/s 0.53: (a) Pure OPC, (b) OPC+6% BaSO<sub>4</sub>, (c) OPC+12% BaSO<sub>4</sub>, (d) OPC+18% BaSO<sub>4</sub>, (e) BaSO<sub>4</sub>. A: Alite B: Belite C: Calcite P: Portlandite Ms: Monosulfate Bs: Barium sulphate

### TG results

TG-DTG curves for OPC- BaSO<sub>4</sub> (0, 6%, 12%, 18%) samples after 28 days hydration are presented in Fig. 3 (a) and (b), respectively. These figures also show the data for pure BaSO<sub>4</sub> for comparison. BaSO<sub>4</sub> did not show any significant features in TG and DTG curves due to its stability up to about 1100 °C of decomposition temperature. The results for OPC obtained in the present study were similar to published curves for OPC pastes [25]. Different events can be seen in DTG curves: the initial weight loss under 100 °C was thought to be from the free water in the system. The peak between 110 °C and 120 °C, peak 3, is the result of the dehydration from C-S-H. Further weight loss at around 180 °C, peak 5, is probably attributed to the dehydration of monosulfate. There was also another peak at around 480°C, peak 6, which is the most significant reaction from the decomposition of Ca(OH)<sub>2</sub> to form calcium oxide. Finally, the wide peak at 650 °C, peak 7, could be due to the decomposition of CaCO<sub>3</sub> and loss of CO<sub>2</sub>.

The TG and DTG curves for OPC- BaSO<sub>4</sub> system with different BaSO<sub>4</sub> loading were similar. There were four distinct stages of weight loss corresponding to the peaks in DTG (peaks 1, 2, 3, 6, and 7). The peaks below 100 °C, peak 1 and 2 correspond to the evaporable free water. The second major peak, peak 3, it was due to the dehydration of C-S-H. The third major peak, peak 6, between 410 °C and 520 °C corresponds to the dehydration of Ca(OH)<sub>2</sub>. The fourth peak between 660 °C and 700 °C, peak 7, corresponds to the decarbonation of calcium carbonate. Smaller peaks were also found in DTG curves. Peak 5, at 180 °C is due to the loss of water from monosulphate phase. The origin of peak 4 at around 120 °C was not clarified and further investigations are required. Table 4 shows the

Ca(OH)<sub>2</sub> content which was calculated by measuring the weight loss between 410 °C and 520 °C. Taylor [25] gives the starting point of Ca(OH)<sub>2</sub> decomposition through dehydration as occurring at 370°C , and it completes by 580°C.

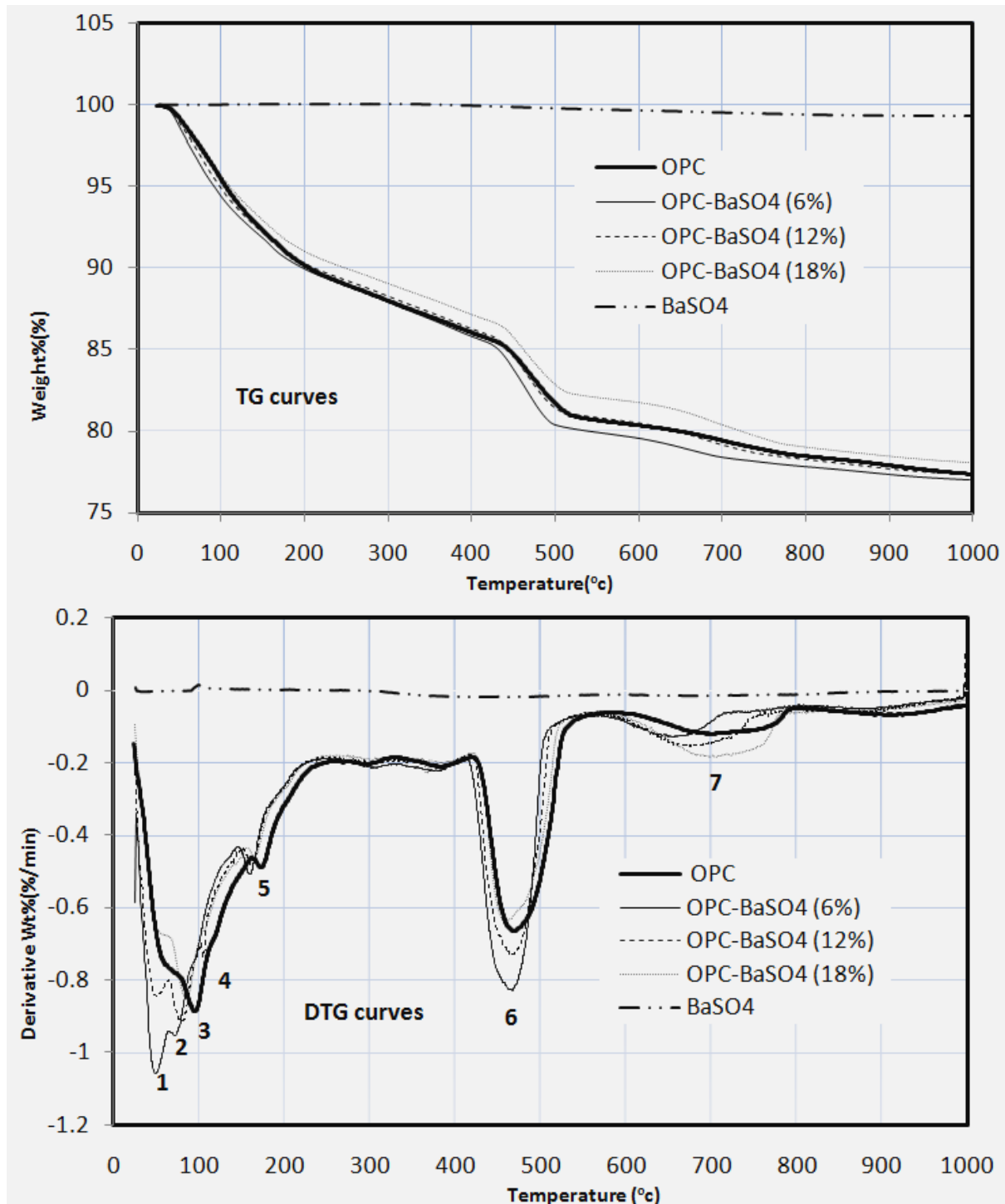


Figure 3 TG and DTG curves for OPC, BaSO<sub>4</sub>, and OPC-BaSO<sub>4</sub> (6%, 12%, and 18%) cured at 40°C for 28 days

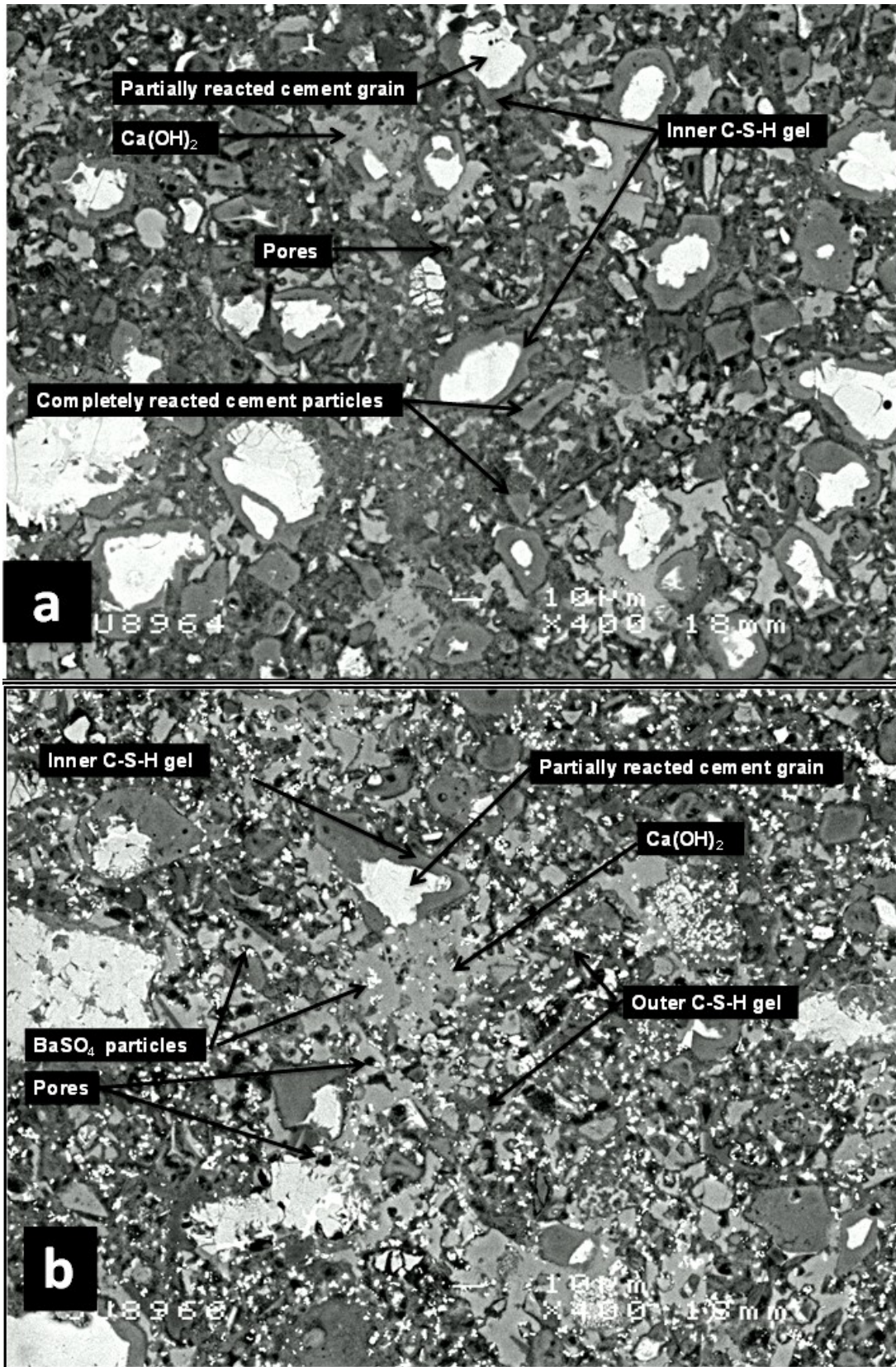
## WM2011 Conference, February 27 – March 3, 2011, Phoenix, AZ

Table 4 Location (°C) of peaks identified in TG results and calculated Ca(OH)<sub>2</sub> content in the OPC-BaSO<sub>4</sub> samples calculated based on the results.

Peak number	Peak	Temperature (°C)	Mass loss, mg		
			OPC-BaSO <sub>4</sub>		
			6%	12%	18%
1	First free water loss	50	-	-	-
2	Second free water loss	80	-	-	-
3	Water loss from calcium silicate hydrates	110-120	-	-	-
5	dehydration of Monosulfate	180	-	-	-
6	dehydration of Ca(OH) <sub>2</sub>	410-520	5.467	5.032	4.665
7	decarbonation of calcium carbonate	660-700	-	-	-

### SEM results

The backscattered electrons images (BEI) of hydrated OPC cement and OPC- BaSO<sub>4</sub> (0, 6, 12, 18%) obtained from SEM analysis are shown in Fig. 4. The microstructure appeared very similar in all OPC- BaSO<sub>4</sub> samples: the anhydrous OPC particles could be seen as the white grains embedded in a darker gray C-S-H matrix; Ca(OH)<sub>2</sub> fills some space surrounding grains shown in a lighter gray. Unreacted cement particles seemed to decrease as the quantity of BaSO<sub>4</sub> within the formulation increased. This agrees with XRD results which indicated the intensity of clear peaks of crystalline barite increased, BEI showed fine particles of BaSO<sub>4</sub> dispersed throughout the microstructure which indicates that the BaSO<sub>4</sub> particles were integrated well within the outer hydration products.



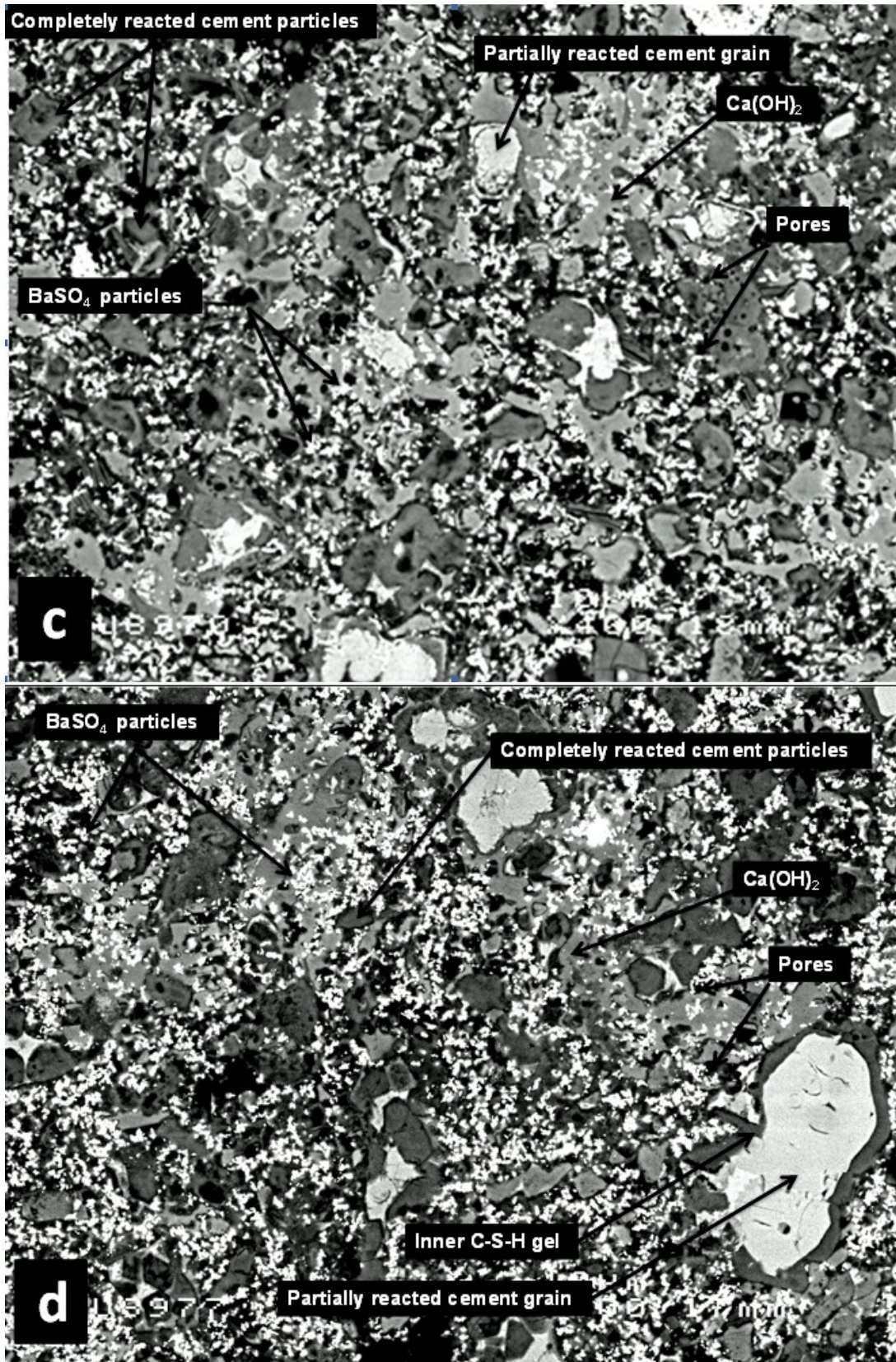


Fig. 4 BSE images of wasteform. (a) OPC, (b) OPC-6% BaSO<sub>4</sub>, (c) OPC-12% BaSO<sub>4</sub>, (d) OPC-18% BaSO<sub>4</sub>

## **CONCLUSION**

In the present study, OPC system with additions of a simulated radioactive waste stream of BaSO<sub>4</sub> with different waste loading (0%, 6%, 12%, and 18%) was studied. The aim of our work was to analyse characteristics and microstructure on cementitious wasteform containing BaSO<sub>4</sub> simulate as a function of waste loading.

The basic cement hydration was not disturbed by addition of BaSO<sub>4</sub> into cement paste up to 18wt%. XRD results indicated that the main crystalline phases detected for hydration of pure OPC for 28 days were calcium hydroxide (P) and Monosulfate (Ms). The XRD traces for samples containing BaSO<sub>4</sub> also indicated clear peaks of BaSO<sub>4</sub> (Bs) in addition to those peaks observed in pure OPC. BSE images showed that the BaSO<sub>4</sub> appears to remain unreacted in all OPC matrixes. In addition, BaSO<sub>4</sub> change the pore structure of the cement paste.

## **REFERENCES**

1. M.S. AL-MASRI and A. ABA, "Distribution of scales containing NORM in different oilfields equipment", *Applied Radiation and Isotopes*, (2005), 63, 457-463.
2. D. READ, B. RABEY, S. BLACK, F.P. GLASSER, C. GRIGG and A. STREET, "Implementation of a strategy for managing radioactive scale", *Minerals Engineering*, (2004), 17, 293-304.
3. J.M. GODOY and R.P dA CRUZ, "<sup>226</sup>Ra and <sup>228</sup>Ra in scale and sludge samples and their correlation with the chemical composition", *Environmental Radioactivity*, (2003), 70, 199-206.
4. M.GAZINEU, C.HAZIN and J.GODOY, "Chemical and minerlogical characterization of waste generated in the petroleum industry and its correlation with <sup>226</sup>Ra and <sup>228</sup>Ra contents", *Radioprotection suppl*, ( 2005), 40, 753-758.
5. M. OMAR, H. ALI, M.P.ABU, K.M.KONTOL and Z.AHMAD, "Distribution of radium in oil and gas industry wastes from Malaysia", *Applied Radiation and Isotopes*, (2004) , 60, 779-782.
6. M. AL-MASRI and H. SUMAN, "NORM waste management in the oil and gas industry : The Syrian experience", *Radioanalytical and Nuclear Chemistry*, (2003), 256, 159-162.
7. J.A VEIL, K.P. SMITH, D. TOMASKO, D. ELCOCK and D.L. BLUNT, "Disposal of NORM-aContaminated Oil Field Wastes in Salt Caverns", Argonne National Laboratory,( 1998).
8. M.S. HAMLATA, S. DJEFFALA and H. KADIB, "Assessment of radiation exposures from naturally occurring radioactive materials in the oil and gas industry", *Applied Radiation and Isotopes*, (2001), 55, 143.
9. SNIFFER, "Identification and assessment of alternative disposal options for radioactive oilfield waste", Genesis Oil & Gas Consultants Ltd , (2005)
10. T. STRAND, "Handling and disposal of NORM in the oil and gas industry", Norwegian Radiation Protection Authority, WM99, (1999).
11. J.H. SHARP, J. HILL, , N. B. MILESTON and E.W. MILLER, " Cementitious Systems for Encapsulation of Intermediate Level Waste", Proc. 9th Int. Conf. on Radioactive Waste Management and Environmental Remediation, ICEM, (2003). Oxford , UK, 2003, 1-9
12. D.CHRISS, "Naturally Occurring Radioactive Materials and Chmical Analysis",USA, Southern University-center for energy and environmental studies,( 2002).
13. L. A . SMITH, "Radioactive-scale formation", *Journal of Petroleum Technology*, (1987), June, 697-706.

## WM2011 Conference, February 27 – March 3, 2011, Phoenix, AZ

14. R.FISHER, “Geologic , geochemical and geographic controls on NORM in produced water from oil, gas and geothermal reservoirs”, The University of Texas at Austin, (1995).
15. M.S. FELLAG and H. KADI, “Precipitate containing norm in the oil industry: modelling and laboratory experiments”, Applied Radiation and Isotopes,( 2003), 59, 95–99.
16. T. F. KRAEMER and D.F. REID, “The occurrence and behavior of radium in saline formation water of the US Gulf Coast region”, Chemical Geology (Isotope Geoscience),( 1984), 2, 153-174.
17. F.W.WILSON, “A guide to naturally occurring radioactive material”, Tulsa , PennWell Publishers, (1994)
18. OGP, “Guidelines for the management of Naturally Occurring Radioactive Material (NORM) in the oil & gas industry”, OGP,( 2008). Report No. 412
19. IAEA, “Radiation protection and the management of radioactiv waste in the oil and gas industry”,Austria : IAEA, (2003), Safety Series No 34.
- 20.D.R. LIDE, “Handbook of Chemistry and Physics”, CRC Press, (1991).
21. F. P.GLASSER, “Progress in the Immobilization of Radioactive Wastes in Cement”, Cement and Concrete Research , (1992), 22, 201-216.
22. M.L.GOUGAR, B.E. SCHEETZ and D.M. ROY, “Ettringite and C-S-H Portland cement phases for waste ion immobilisation,a review”, Waste Management, (1996), 16, 295-303.
23. C.UTTON, “The encapsulation of a BaCO<sub>3</sub> waste in composite cements”, PhD Thesis., University of Sheffield, (2006).
24. H.F.W. AYLOR, “Chapter 1: Portland cement and its major constituent phases”, in “Cement chemistry”, Thomas Telford Publishing, London, (1990), 1-28.
25. H.F.W. AYLOR, “Chapter 7: Hydration of Portland cement”, in “Cement Chemistry”, Thomas Telford Publishing, London, (1990), 1-28.